20 janvier 1997

LPCC 97-01
GANIL P 97 01
LYCEN/9703

IPNO-DRE-97-02
SUBATECH-97-02
DAPNIA/SPhN 97-09

Thermodynamical properties and deexcitation of sources involved in collisions between light nuclei around 100 AMeV incident energy

B. Borderie, F. Gulminelli, M.R. Rivet, D. Doré, A. Chbihi et al,

Invited paper at Int. Workshop on Heavy Ion Physics at Low, Intermediate and Relativistic Energy with 4π Detectors, Poiana Brasov, Romania, 7-14 October 1996

THERMODYNAMICAL PROPERTIES AND DEEXCITATION OF SOURCES INVOLVED IN COLLISIONS BETWEEN LIGHT NUCLEI AROUND 100 AMeV INCIDENT ENERGY

B. Borderie[1], F. Gulminelli[2], M.F. Rivet[1], D. Doré[1], A. Chbihi[3], D. Durand[2], Ph. Eudes[6], M. Parlog[1a], L. Tassan-Got[1], G. Auger[3], Ch.O. Bacri[1], J. Benlliure[3], E. Bisquer[4], R. Bougault[2], R. Brou[2], J.L. Charvet[5], J. Colin[2], D. Cussol[2], R. Dayras[5], E. De Filippo[5], A. Demeyer[4], P. Ecomard[3], D. Gourio[6], D. Guinet[4], R. Laforest[2], P. Lautesse[4], J.L. Laville[6], L. Lebreton[4], J.F. Lecolley[2], A. Le Fèvre[3], T. Lefort[2], R. Legrain[5], O. Lopez[2], M. Louvel[2], N. Marie[3], V. Métivier[2b], L. Nalpas[5], A. Ouatizerga[1], J. Péter[2], E. Plagnol[1], A. Rahmani[6], T. Reposeur[6], E. Rosato[3c] F. Saint-Laurent[3], M. Squalli[1], J.C. Steckmeyer[2], B. Tamain[2], E. Vient[2], C. Volant[5], J.P. Wieleczko[3]

[1] *Institut de Physique Nucléaire,IN2P3-CNRS, 91406 Orsay Cedex, France*

[2] *LPC, IN2P3-CNRS, ISMRA et Université, 14050 Caen Cedex, France*

[3] *GANIL, CEA, IN2P3-CNRS, B.P. 5027, 14021 Caen Cedex, France*

[4] *IPN Lyon, IN2P3-CNRS et Université, 69622 Villeurbanne Cedex, France*

[5] *CEA, DAPNIA/SPhN, CEN Saclay, 91191 Gif sur Yvette Cedex, France*

[6] *SUBATECH, IN2P3-CNRS et Université, 44072 Nantes Cedex 03, France.*

Vaporization events, where all species have atomic numbers lower than 3, and deexcitation properties of quasi-projectiles involved in binary dissipative collisions between ^{36}Ar and ^{58}Ni are studied with the multidetector INDRA. Kinematical properties and chemical composition (mean values and variances) of vaporizing sources are derived over the excitation energy per nucleon range 8-28 MeV. These data are found in good agreement with the results of a model describing a gas of fermions and bosons in thermal and chemical equilibrium, which strongly suggests that thermodynamical equilibrium has been reached even for such sources produced in very extreme conditions of collisions. Finally, removing the constraint on atomic numbers lower than 3, the evolution of the chemical composition of quasi-projectiles is presented over the excitation energy range 0-25 AMeV.

1 Introduction

The question of whether or not hot nuclear matter formed in violent heavy-ion collisions reaches thermodynamical equilibrium (thermal+chemical) before starting to disassemble is of essential importance in validating the hypotheses assumed in statistical models[1,2,3] and in constraining the ingredients enter-

[a] permanent address: *Institute of Physics and Nuclear Engineering, IFA, P.O. Box MG6, Bucharest, Romania*

[b] present address: *SUBATECH, IN2P3-CNRS et Université, 44072 Nantes Cedex 03, France*

[c] permanent address: *Dipartimento di Scienze, Univ. di Napoli, 80125 Napoli, Italy*

ing microscopic models based on transport theories[4,5,6,7]. Moreover a positive answer to this question renders appropriate the application of physical concepts borrowed from macroscopic statistical mechanics like phase coexistence and phase transition. In particular, chemical equilibrium controls the yields of the different products and strongly influences their isotopic composition. Therefore, the experimental study of such an issue requires the detection and identification (mass and charge) of all or nearly all deexcitation products. This kind of measurement was recently achieved by studying with INDRA[8] a particular class of events produced in $^{36}Ar+^{58}Ni$ collisions, namely the vaporization events[9]. These events, where more than 90% of the charged particles were detected and isotopically identified, were properly characterized since the total number of - unmeasured - neutrons could be derived event by event from mass conservation. The vaporization events, which were studied at 52,74,84 and 95 AMeV incident energies, are produced in binary dissipative collisions. At the higher bombarding energy a broad excitation energy range (6-28 AMeV) is observed for the two partners of collisions (quasi projectile: QP and quasi target: QT)[10]. Thus, the possible occurrence of thermodynamical equilibrium can be studied in very extreme conditions of collisions (conservation of the binary character of collisions and very large excitation energies involved).

2 Properties of vaporizing sources

2.1 Excitation energies

To correctly derive the properties of these sources, the dynamics of the collisions must first be studied: are we dealing with the vaporization of one source, or of several sources? The details given in [10] indicate the dominance of collisions with two partners in the exit channel. Only a very small part of the events (whatever the incident energy) could possibly be associated with the decay of a single source and were not included in the analysis. Usually, for heavy systems, the source reconstruction makes use of the heaviest products only. In a similar way, the subset of particles with masses larger than 2 was used here. These particles carry on average more than 50% of the total mass of the system. Different methods (see [10]) were used to determine the source velocities and it was verified that they yield similar results. The spectra of the relative velocity between the sources were found very broad. An example of spectrum is shown in the upper part of Fig 1; vertical lines refer to projectile velocity and relative velocity between the two partners due to coulomb repulsion.

The primary masses and the excitation energies of the two sources were obtained by first including the measured particles not considered in the recon-

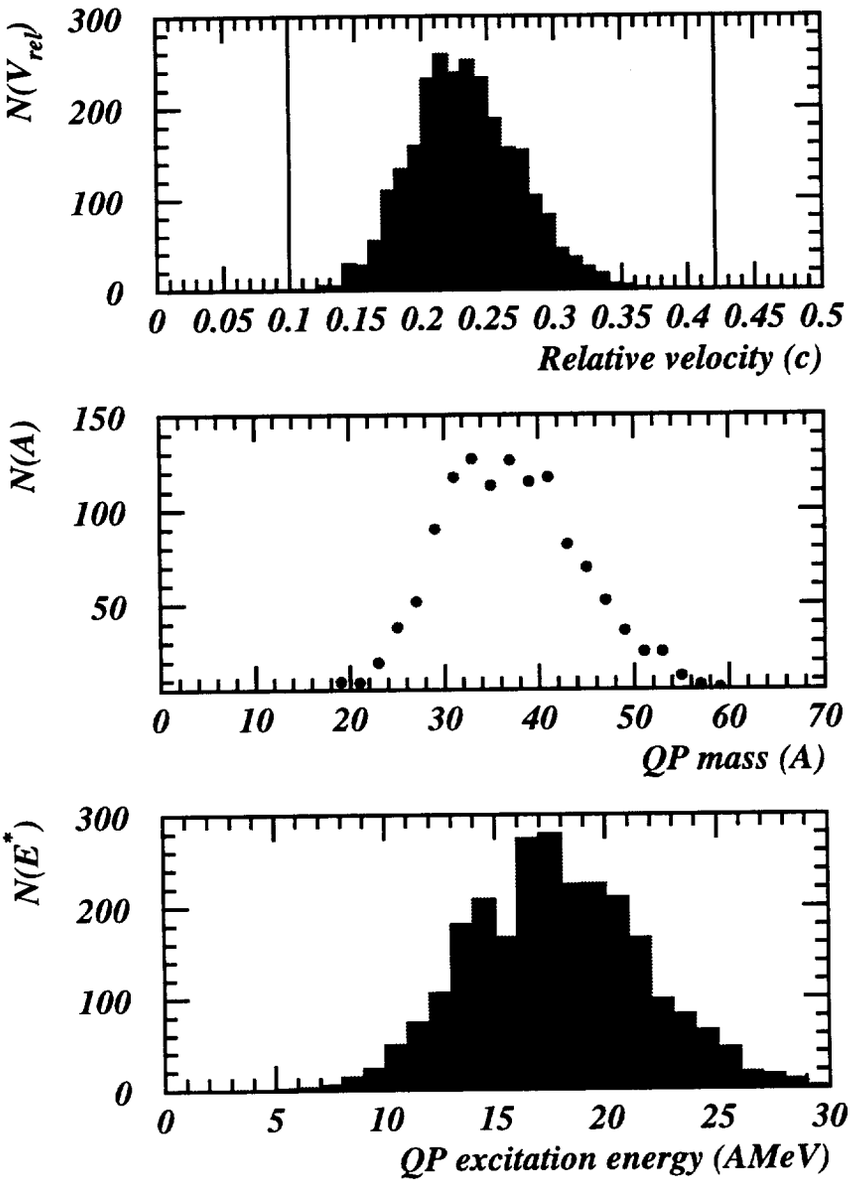

Figure 1: Properties of QP at 95 AMeV incident energy. Top: relative velocity distribution between QP and QT. Middle: initial mass distribution for the QP. Bottom: excitation energy distribution for the QP.

struction of the sources (p and d); they were attributed to the source in which their relative velocity is smallest. Then, each event is completed in charge according to the measured particle distribution, and all added charged particles are attributed to the slower source, assuming that the effects of the detection thresholds overcome those of the geometrical efficiency. Finally total neutron multiplicity then follows from mass conservation; the forward source is completed to $N = Z + 1$ whenever its measured neutron number is smaller, the remaining neutrons are put in the backward source. The kinetic energies of the added charged particles are taken equal to the average energy of the same particle species in the events belonging to the same excitation energy bin; for neutrons one uses the average proton energy minus 2 MeV to take into account the Coulomb barrier. At all energies, the source masses are found to be close (38 and 56) to the initial projectile and target masses but with large fluctuations ($\sigma \sim 8$). In the following the sources will then be called quasi-projectile (QP) and quasi-target (QT). The excitation energy of each source is calculated as [11]

$$E_S^* = \sum_i (\Delta m_i + E_{Ki}) - \Delta m_S, \tag{1}$$

Δm_i being the mass excess of particle i, Δm_S that of the source, and E_{Ki} the ith particle kinetic energy in its source frame. As expected from the broad spectra observed for the relative velocities between the sources and for the QP and QT masses, the distributions of the excitation energy per nucleon of each source are also very broad. Fig 1 summarizes the data obtained at 95 AMeV for the QP. From the reconstruction of the total energy we can estimate at 2 AMeV the resolution of the calculated excitation energy per nucleon.

2.2 Kinematical properties and composition

Whether or not each vaporizing source reaches thermal or thermodynamical (thermal and chemical) equilibrium before disintegrating can be investigated by looking at the energy spectra and relative abundances of the different particles in each source [12] , as a function of its excitation energy per nucleon, ϵ^*; a binning $\delta\epsilon^*$=3MeV was chosen. We discuss first the shapes of the kinetic energy spectra, in the source frames, which give information about thermal equilibrium for each source.

First it was checked that the forward and backward spectra are superimposable (see Fig 2). Spectra, integrated over angle, are structureless, with exponential tails whose slopes are similar within 30% for all particles. More quantitatively, for the emission from a source in thermal equilibrium, all par-

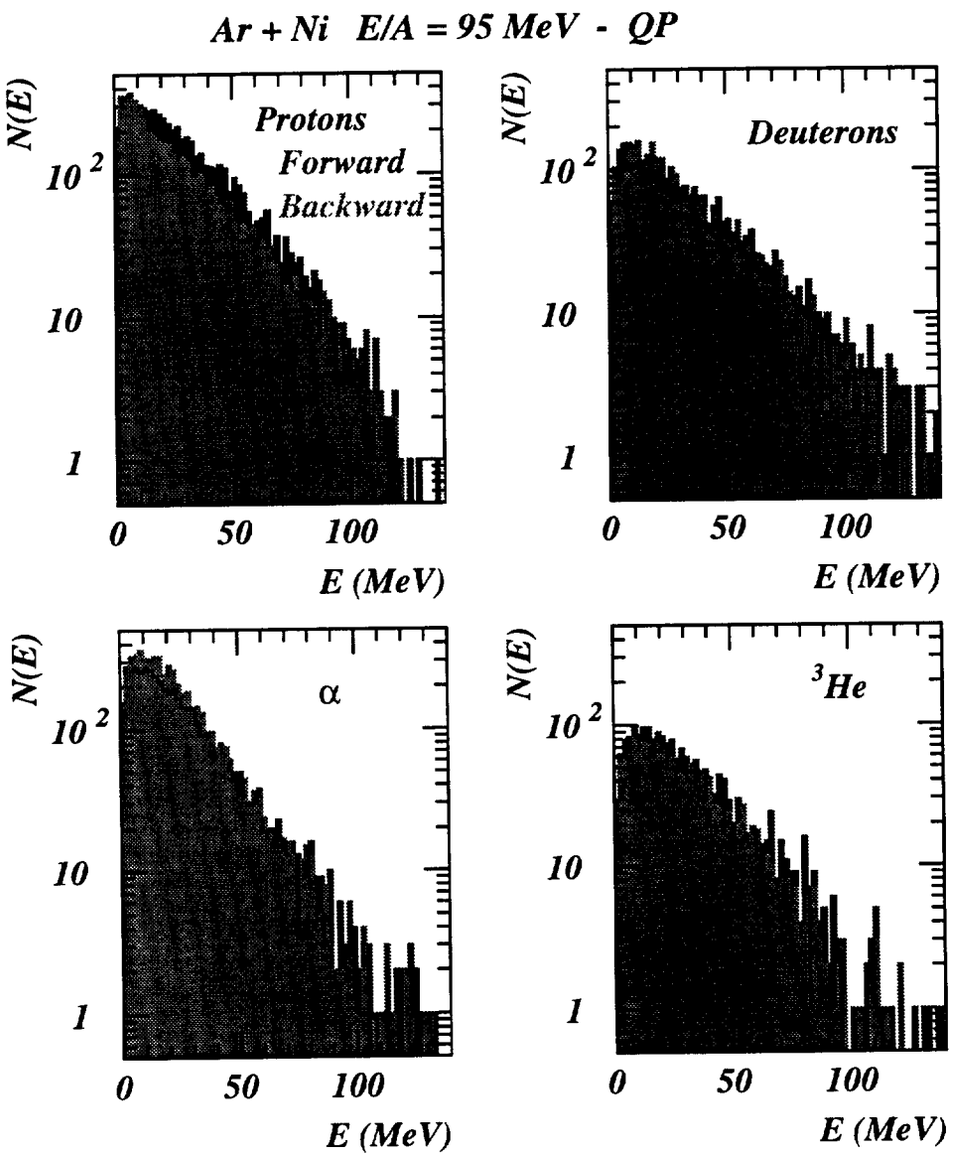

Figure 2: Forward and backward energy spectra of particles emitted by the QP (in the QP frame).

ticles should have the same average kinetic energy if we neglect in a first approximation the Coulomb barrier. The increase of the average kinetic energy with the excitation energy is almost linear for all particles [12]. An example of the evolution of the average kinetic energy of each particle species is given in Fig 3 (bottom part), for the QP at ε^*=18.5 MeV (identical values are obtained for the QT); a difference of ~20% is observed here and exists over the whole excitation energy range between the more energetic particles (d and ^3He) and the less energetic ones (p and ^4He). This may appear as a significant deviation from thermal equilibrium. Since no extra collective expansion energy (proportional to the atomic mass) can be derived from the data, the role of quantal effects and side-feeding has to be checked.

We now come to the chemical composition of the vaporized sources. In Fig 3 (upper part) is shown the relative particle abundance ($P_j = M_j/M_S$, where M_S is the total source multiplicity and M_j the multiplicity of particle species j in the source) versus the source excitation energy, for the QP at 95 AMeV. α-particles dominate at the lower excitation energies, while protons take over when the excitation energy is increased. The deuteron relative abundance is roughly constant; the isobars of mass 3 have opposite behaviours: tritons slightly decrease and ^3He increase when raising the energy. This evolution is not due to autocorrelations between the source composition and its excitation energy. Indeed, the mass balance part accounts for ~ 40% of the excitation energy around 10 AMeV, and only 20% around 22 AMeV. Therefore the increase of the source excitation energy is not only due to the increase of the nucleon abundance, but also to the increase of the kinetic energy of the particles. Note that for a given ε^* the relative yields are the same for the QP and the QT, independently of the bombarding energy.

2.3 Comparison with a model

2.3.1 Mean energies of particles and chemical composition

In the model [13] , which is expected to be well suited to describe the situation discussed here, the emitting source is viewed as a nuclear gas of fermions and bosons in thermal and also chemical equilibrium. For a given source density ρ and temperature T, the energy spectra $n_i(E)$ of the different nuclear species (and consequently their relative yields) are uniquely determined from conservation laws and the equilibrium distributions in the grandcanonical ensemble

$$n_i(E) = f_Q(E, \mu_i, T) \;\; i = 1, \ldots N \qquad (2)$$

where N is the number of species taken into account (limited here to nuclear states which deexcite in Z=0,1,2, up to ^{20}Ne) , f_Q is the density of occupied

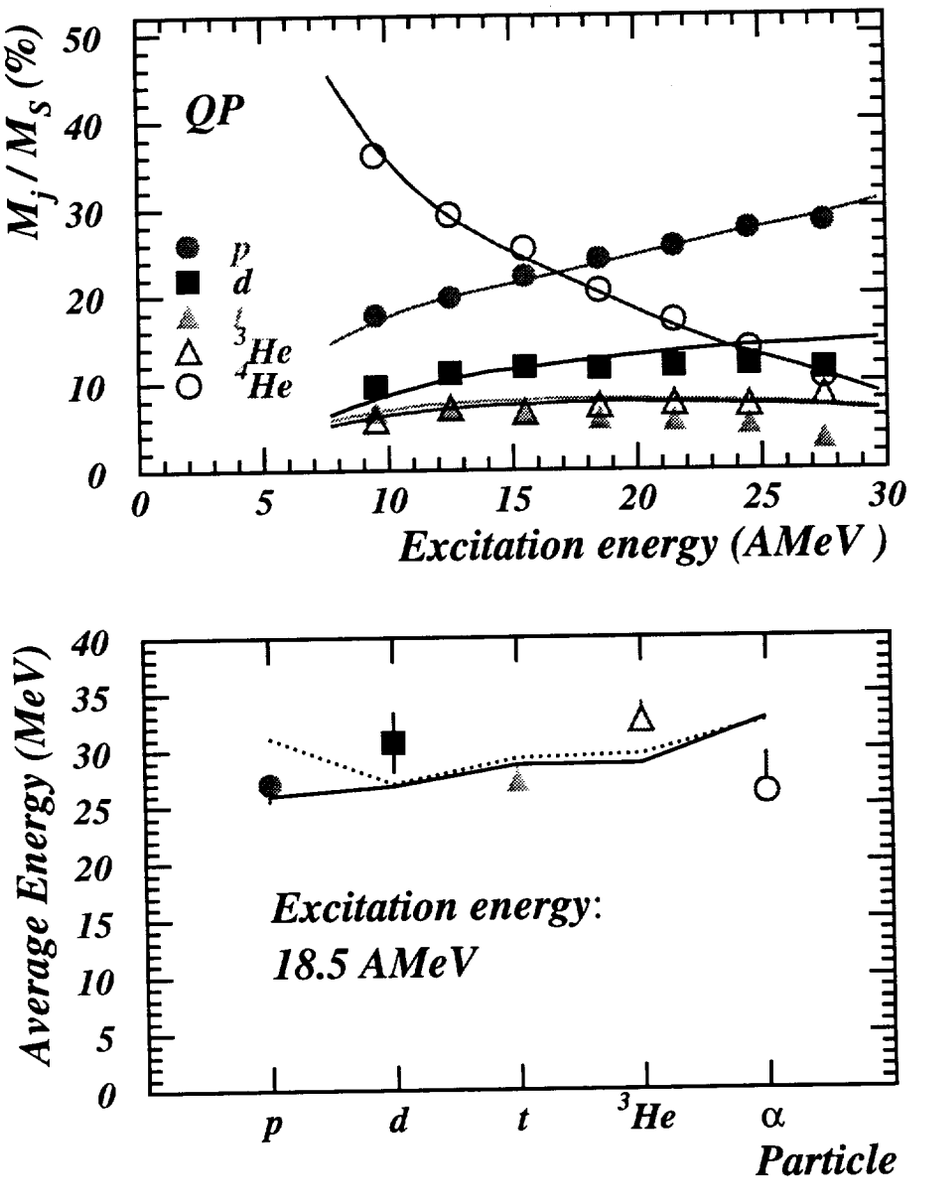

Figure 3: Bottom part: average kinetic energies of particles emitted by the QP with an excitation energy per nucleon of 18,5 MeV. Upper part: composition of the QP as a function of its excitation energy. Symbols are for data while the lines are the results of the model (see text).

states taking into account the appropriate quantum statistics (Fermi or Bose) and μ_i is the chemical potential of the species i, which is a function of the break up density ρ via the neutron and proton chemical potentials μ_N, μ_Z

$$\mu_i = \mu_N N_i + \mu_Z Z_i + B_i \tag{3}$$

Here, N_i, Z_i are the neutron and proton numbers of the isotope under consideration and B_i its binding energy. All excited states with a width smaller than 1 MeV are taken into account, and the final distributions are corrected for the side-feeding of resonance decay. Corrections to the ideal gas are also included in the form of excluded volume effects. The consequence of the excluded volume is to favour protons,neutrons and alphas over the more loosely bound structures like deuterons and high-lying resonances [13]. In this calculation ε^* is derived, as in the experiment, by summing the kinetic energies of all particles and the Q value. The experimental ε^* range is covered by varying T from 10 to 25 MeV. The freeze-out density has been fixed to $\rho = \rho_0/3$, in order to reproduce the experimental ratio between the proton and alpha yields. The results of the model correspond to the lines in Fig 3.

The average kinetic energies of the different particles are rather well reproduced particularly for protons, but the model fails to accurately follow the dependence on the different species. The energy differences between particles in the model are due to the different statistics (Fermi or Bose) and to side-feeding. This last effect, which depends on the number of species included in the model, does not influence much the calculated values. To illustrate this point, the dashed line in Fig 3 corresponds to results with species limited to excited ^9B. Experimental error bars in the figure give the limits obtained when methods which use all the particles for reconstructing the sources are applied.

The yields of the different species as a function of the excitation energy (see Fig 3 top) are very well reproduced, especially below ε^*=25 MeV.

2.3.2 Variances of the multiplicity distributions

As discussed earlier the model has one free parameter: the freeze-out density, which was fixed using the ratio of proton and alpha yields. To be more convincing on the fact that thermodynamical equilibrium has been reached, it is necessary to compare not only the mean values, but also the second moments of the distributions, i.e. the variances associated with the multiplicities of the different particles [14]. To do this, we have to take into account the complexity concerning the fluctuations involved in the collisions. On the thermal fluctuations that we want to measure are superimposed dynamical fluctuations related to the reaction mechanism. In the experiment we have verified that the variances of multiplicity distributions are independent of the width of the excitation energy bin considered (from 1 to 3 MeV). Moreover in the

model, the mass distributions of the source associated with different excitation energy bins and the total excitation energy distribution were used as inputs. Thus a Monte Carlo simulation starting with the calculated partition function produces events which are analyzed like the data. The comparison data-calculations is displayed in Fig 4 for the different variances associated with the total multiplicity and with those of proton and alpha. A good agreement is observed, which strongly supports the fact that thermodynamical equilibrium has been reached for such sources before deexcitation.

3 Deexcitation of quasi-projectiles

Removing the constraint on atomic numbers lower than 3 and the selection of events where more than 90% of the total charge of the system was detected, deexcitation properties of QP have been derived after the use of a completion method.

3.1 Selection of events and completion method

From observations of correlations between the total detected charge, the total multiplicity of charged products and the total parallel momentum (calculated with charge instead of mass)[9], it was possible to select events for which almost all particles associated with the QP have been well detected: a double selection was applied keeping events for which i) the sum of the charges of all detected products was larger than the atomic number of the projectile (18) and ii) the total parallel momentum was larger than 70% of the projectile linear momentum. Then the completion method consists in adding, in an event by event analysis, a fragment whose charge and momentum amount to the missing corresponding quantities; the values so derived for the emission angle, the kinetic energy and the charge of the added fragment, are in good agreement with energy thresholds, geometrical efficiency and the hypothesis to have missed fragments emitted from quasi-targets. Then a complete analysis as described in 2.1 was performed to extract the QP properties over the ϵ^* range 0-25 MeV.

3.2 Deexcitation properties

Fig 5 summarizes the evolution of the deexcitation properties as a function of ϵ^*, the mass of the QP varying from 35 to 30 when ϵ^* covers the range 0-25 MeV. A fragment is defined as a species with atomic number larger than 2. The upper part of the figure shows the different probabilities for n-fragment emission. One-fragment emission, which decreases slowly when the excitation

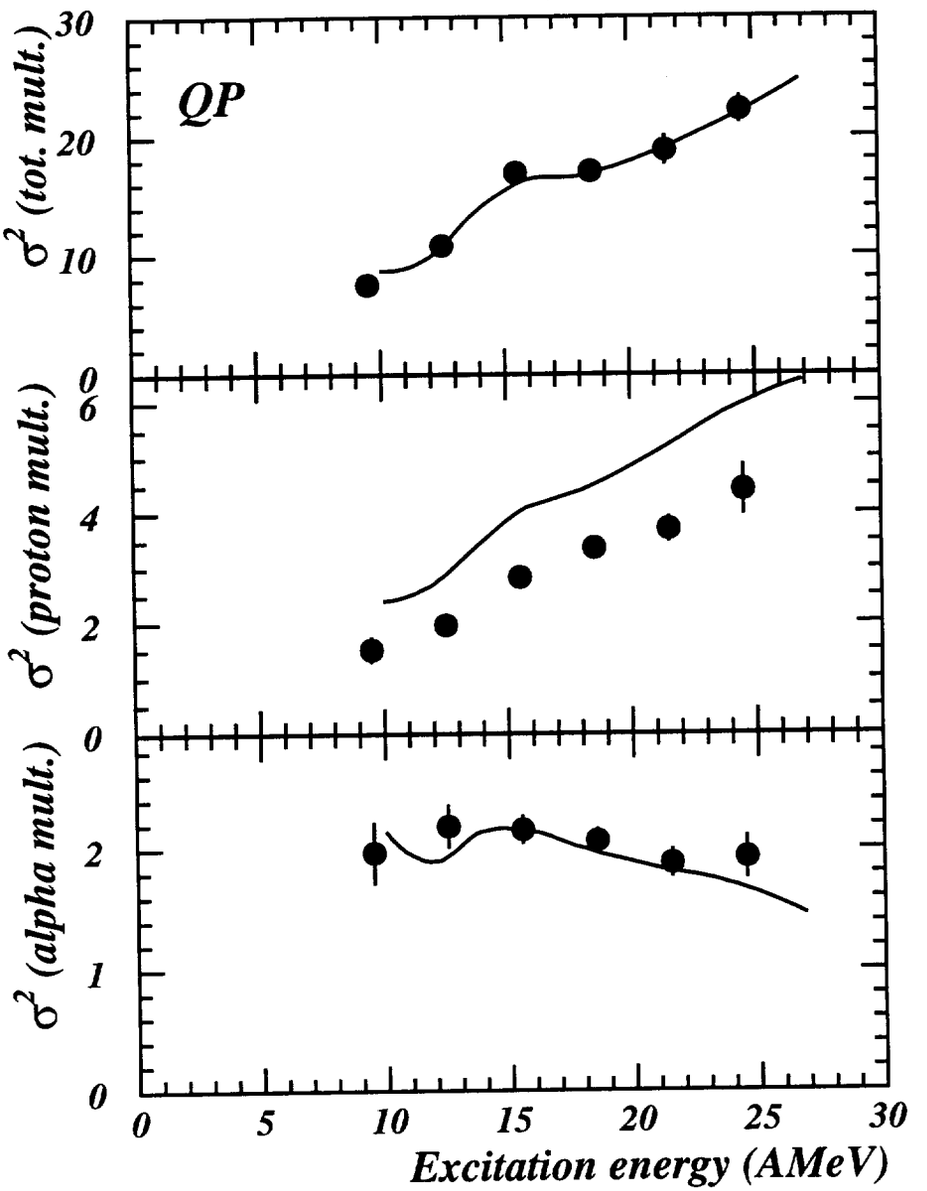

Figure 4: Variances of multiplicity distributions (total, proton and alpha) of the QP as a function of its excitation energy per nucleon. Points refer to the data and the lines are the results of the model (see text).

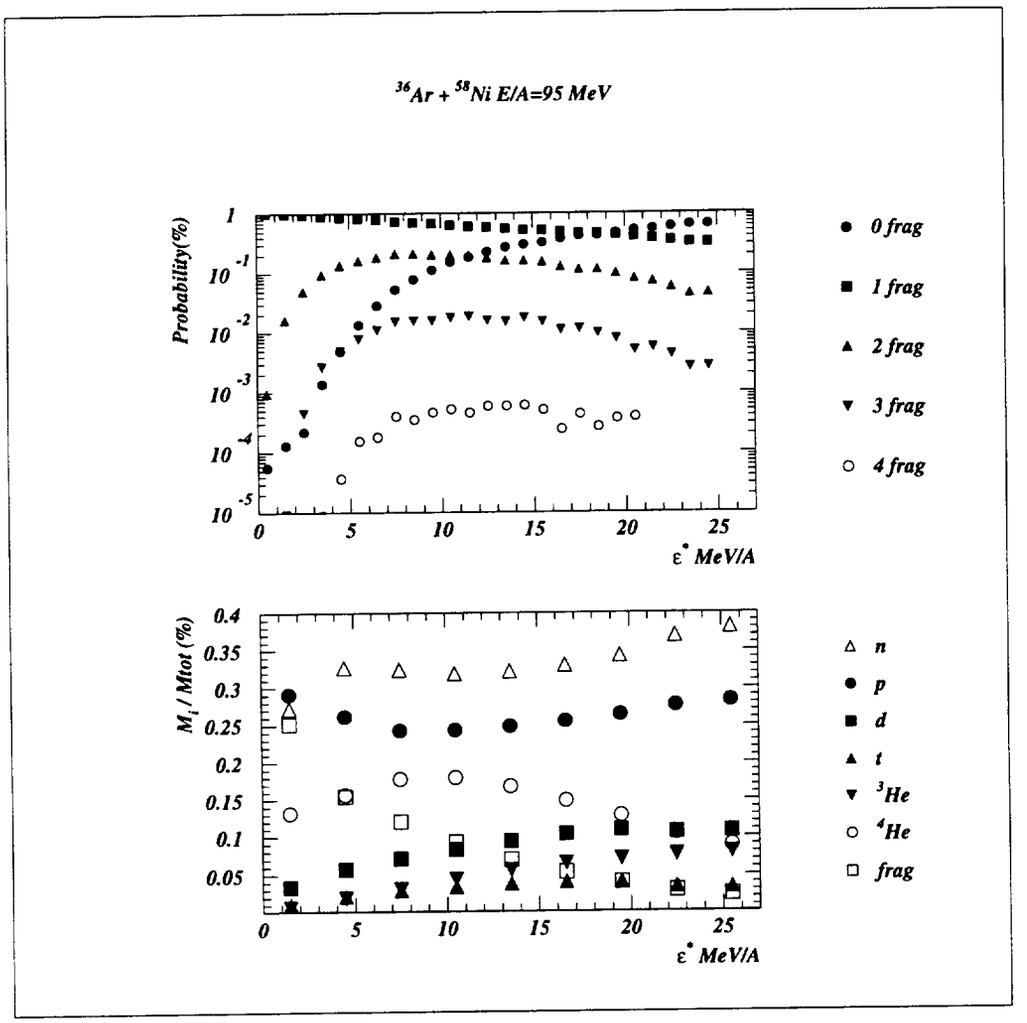

Figure 5: Deexcitation properties of the QP as a function of its excitation energy

energy increases, dominates until around 15 MeV. At higher energy the vaporization of the QP becomes the dominant process. The probability to emit 2,3 and 4 fragments is rather constant over the range 7-15 MeV. The lower part of the figure, which indicates the evolution of the relative particle abundance versus the source excitation energy, exhibits for protons and alphas a reversing of the slope around 8-10 MeV. This appears as correlated to the change from evaporation to multifragmentation regime as discussed in [13,15].

Work is now in progress to compare these very complete data, as well as the evolution of the Z distributions as a function of ε^* not presented here,

with models related to evaporative regime, multifragmentation models and the model proposed here.

For the light system studied here, we can estimate that around 30% of the events do not correspond to pure binary collisions. These events are polluted by fragments and particles detected around mid-rapidity [15]. However a more careful selection of the events does not significantly modify the results presented in Fig 5.

4 Conclusions

Emission properties of vaporizing sources produced in collisions between ^{36}Ar and ^{58}Ni have been studied in a broad excitation energy range . The yields (mean values and variances) and the energy spectra of the different species have been compared with the predictions of a model describing the properties of a gas of fermions and bosons in thermal and chemical equilibrium. All these experimental observables are rather well reproduced, which give strong confidence in the fact that thermodynamical equilibrium has been reached for sources produced in very extreme conditions. Finally very complete data, concerning the deexcitation of a source of mass 30-35, over the excitation energy range per nucleon 0-25 MeV, have been presented. These new data would help us to understand the transition from the well known evaporative regime to the multifragmentation one in terms of fundamental properties of nuclear matter.

References

1. J. Bondorf et al, *Nucl. Phys.* **A443** (1985) 321, **A444** (1985) 460, **A448** (1986) 753.
2. D.H.E. Gross, *Rep. Prog. Phys.* **53** (1990) 605. and references therein
3. H. Stocker and W. Greiner, *Phys. Rep.* **5** (1986) 277
   J. Konopka et al, *Phy. Rev.* **C50** (1994) 2085.
4. G. Bertsch and S. Das Gupta, *Phys. Rep. 160 (1988) 189*
5. J. Aichelin, *Phys. Rep. 202 (1991) 233*
6. A. Bonasera, F. Gulminelli, J. Molitoris, *Phys. Rep. 243 (1994) 1*
7. D.Idier et al, *Ann. Phys. Fr. 19 (1994) 159*
8. J. Pouthas et al, *Nucl. Instr. Meth. in Phys. Res.* **A357** (1995) 418, **A369** (1996) 222.
9. C.O. Bacri et al, *Phys. Lett.* **B353** (1995) 27.
10. M.F. Rivet et al, *Phys. Lett.* **B388** (1996) 219.
11. D. Cussol et al, *Nucl. Phys.* **A561** (1993) 298.
12. B. Borderie et al, *Phys. Lett.* **B388** (1996) 224.

13. F. Gulminelli and D. Durand, LPCC report 96-11 and *Nucl. Phys.* in press.
14. B. Borderie et al, to be published
15. J. Péter et al, this Workshop.